RSC Advances

PAPER

View Article Online
View Journal | View Issue

Cite this: *RSC Adv.*, 2017, **7**, 46344

Some new azobenzene liquid crystals involving chalcone and ester linkages†

Xueyou Zhu, Fengnan Yin, Haiying Zhao,* Shufeng Chen and Zhanxi Bian

Received 22nd June 2017
Accepted 26th September 2017

DOI: 10.1039/c7ra06958h

rsc.li/rsc-advances

Five new series of azobenzene derivatives containing thiophene, naphthalene or ferrocene with chalcone and ester linkages have been synthesized and characterized. The photosensitive azobenzene group underwent photoisomerization under UV light, which was monitored by UV-visible spectroscopy. The cyclic voltammograms of compounds containing ferrocene showed a quasi-reversible and diffusion-controlled redox process. These compounds displayed high thermal stability according to the thermogravimetry measurements. According to differential scanning calorimetry, thermal polarizing microscopy and powder X-ray diffraction studies, the compounds containing ferrocene and the compounds with three or no terminal alkoxy chains on the side of the ester group all showed no liquid crystal behaviour. However, the compounds with a terminal alkoxy chain on the side of the ester group or a terminal alkoxy chain at both ends of the molecule exhibited enantiotropic mesophases, but the latter had a narrow mesogenic domain. The increase of the length of the mesogenic unit by replacement of the benzene ring with a naphthalene ring resulted in both an increase in the clearing point and in an increase in the mesophase domain.

1 Introduction

Thermotropic liquid crystals (LCs) are a special category of soft matter; their molecular order and dynamics are intermediate between an isotropic fluid and that of a crystal.[1] LC materials are promising candidates for fabricating cost-effective and portable bio/chemical sensors, and for interfacial and opto-electronic applications.[2–4] A thermotropic liquid crystal consists of either linear or disclike molecules. The general architecture for linear thermotropic liquid crystals consists of linearly linked ring systems and flexible chains. The rings may be linked to each other either directly or through some linking group (*e.g.* ester, olefinic, acetylenic, azo, imido) that maintains the linearity of the core.[5] Azobenzene, as one of the traditional photochromic moieties, is thermally very stable and can perform photo-induced reversible isomerization under UV irradiation,[6–10] So azo compounds have advantages over substances with other linkages like ester, tolane or even the more commonly encountered Schiff's base linkage.[11–13] In recent decades, azobenzene based low and high molecular weight liquid crystalline materials have been frequently discussed for their sensitivity of chromophoric group towards light and found to exhibit interesting optical properties, which enable us to study the materials in holography, optical storage device, optical switching and establish widespread applications in display technology.[14–19]

On the other hand, chalcones are the main precursors for the biosynthesis of flavonoids and isoflavonoids. A variety of organic molecules with chalcone moiety have been evaluated for pharmacological applications due to their good antimicrobial,[20] nematocidal,[21] anticancer[22] and antiplasmodial[23] activities. In addition, chalcones are reported to be effective photosensitive materials and have potential nonlinear optical[24] and liquid crystal properties.[25] Chalcone linkage along with other linkages, such as imine and ester groups, combined to exhibit various mesophases.[26–31] However, to the best of our knowledge, there are rare reports about the combination of azo and chalcone linkages using in the liquid-crystalline materials to date.[32,33] In this article, we synthesized a series of new liquid crystalline compounds involving chalcone, azo and ester linkages. The designed molecular structures are shown in Fig. 1. Their redox and optical properties were studied. Thermometric data will be evaluated in terms of molecular rigidity and flexibility depending on molecular structure and then mesomorphic properties and behaviors will be compared with structurally similar series.

Inner Mongolia Key Laboratory of Fine Organic Synthesis, College of Chemistry and Chemical Engineering, Inner Mongolia University, Hohhot 010021, China. E-mail: hyzhao@imu.edu.cn

† Electronic supplementary information (ESI) available: Detailed procedures of synthesis and characterization of compounds **VIa–VIe**, Tables SI–SII, Fig. S1–S30. See DOI: 10.1039/c7ra06958h

2 Results and discussion

2.1 Photoisomerisation studies

The photoisomerisation studies were carried out on the selective compounds dissolved in the dichloromethane. The initial

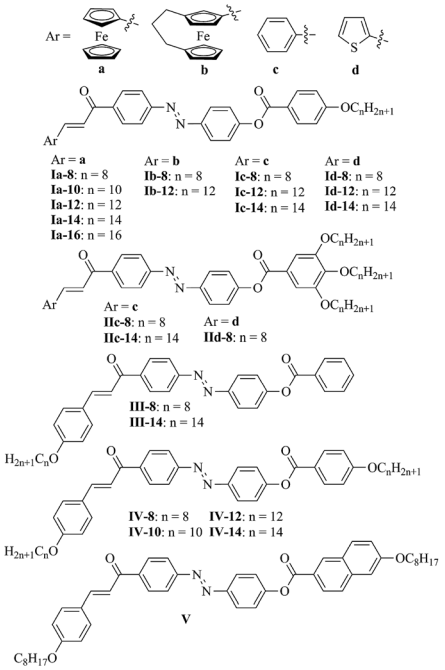

Fig. 1 The structures of compounds I–V.

measurements were carried out on the unexposed materials. The obtained results of the UV-visible absorption spectra (UV-vis) are presented in Fig. 2 and Table S1.†

Compounds **Ia-8** and **Ib-8** exhibited three absorption bands, whereas others exhibited two absorption bands. The absorption bands in ultraviolet area were attributed to the π–π* electronic transitions. For the compound **V**, the absorption band centered at ~260 nm (see Fig. 2 insert) had large molar absorption coefficient after introducing the naphthalene ring. The absorption due to Fe(d)-π* electronic transitions in compounds **Ia-8** and **Ib-8** also appeared at the range of 260 nm. In addition, the same absorption at 346 nm for compounds **Ia**, **Ib** and **Ic** indicated that the introduction of ferrocenyl almost had no effect on this absorption. However, this band shifted bathochromically about 10 nm after introduction of thiophene ring (compounds **Id** and **IId**) or alkoxy group on the side of chalcone (compounds **III**, **IV** and **V**). Furthermore, compounds **Ia-8** and **Ib-8** with ferrocenyl showed very broad absorption bands at 480–620 nm due to d–d type transitions of the electrons of the iron atoms, and this band for the [3]ferrocenophane-containing **Ib-8** was stronger than that of ferrocene-containing **1a-8**.[34]

Next, the compounds were irradiated with UV light (365 nm). As an example, the spectral changes of **Ic** are presented in Fig. 3. With increasing time of irradiation the band at 342 nm strongly decreased. This change in the UV-vis spectrum suited the reduction of concentration of *E* isomers in azo group in irradiated mixture. At the same time, the increase of the band at 440 nm (n–π* electron transition) corresponded to the growth of the concentration of *Z* isomer in azo group in investigated mixture. Moreover, the equilibrium between *Z* and *E* isomers in azo group was established after 75 s of irradiation. The isosbestic points were observed at 312 and 408 nm, corresponding

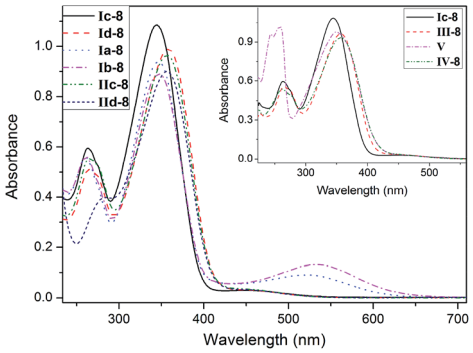

Fig. 2 UV-vis absorption spectra of selective compounds I–V taken at 10^{-5} M in CH_2Cl_2.

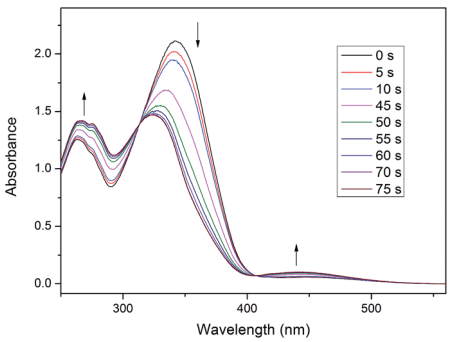

Fig. 3 Changes of absorption spectra of **Ic-8** in CH_2Cl_2 during UV exposure.

to *E*–*Z* isomerization as these suggesting that only two isomers obtained. Furthermore, another absorption band exhibited chalcone unit in double bond underwent isomerization around 263 nm.[35] Table 1 shows the summary of time taken for the selected compounds for *E*–*Z* photoisomerisation with their calculated conversion efficiency (CE).[7] As shown in Table 1, **1a-8** took the longest time (157 s) for *E*–*Z* conversion with the CE of 27.3% after exposure to UV light, whereas **Ic-8** gave 45.1% of CE when bulky ferrocene was replaced by a benzene ring. However, **Id-8**, **IV-8** and **V-8** took shorter time (40–50 s) with the low CE of 8–10% after introducing alkoxy chain in benzene ring. The possible reason is the bulky ferrocene and alkoxy chain increasing the energy of *Z* isomer.

After irradiation samples were left in the dark to allow thermal back relaxation. This process for **Ic-8** is presented in Fig. 4. It can be seen that back transition from *Z* to *E* form was much slower than the isomerisation during the UV irradiation, and the equilibrium for compound **Ic-8** was not achieved yet after 1485 min. Similar phenomena were observed in other compounds. Long thermal back relaxation allows us to realize that optical storage devices with these materials which need longer periods.

2.2 Electrochemical investigation

The electrochemical properties of representative compounds containing ferrocene (**Ia-8**, **Ia-12** and **Ib-12**) were studied by

Table 1 Time taken for the azo derivatives for *E*–*Z* isomerisation with their calculated conversion efficiency

Compd.	*E*–*Z* (time) (s)	CE (%)
Ia-8	157	27.3
Ic-8	75	45.1
Id-8	40	9.6
IV-8	50	10.2
V-8	40	8.7

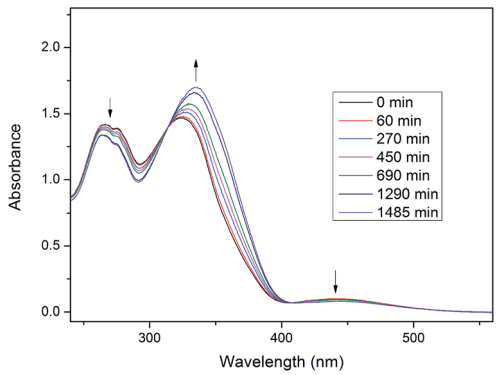

Fig. 4 Changes of absorption spectra of **Ic-8** in CH_2Cl_2 during thermal back relaxation.

cyclic voltammetry (CV) using CH_2Cl_2 as the solvent containing 0.1 M tetra-*n*-butylammoniumhexafluorophosphate ($TBAPF_6$) as a supporting electrolyte. Electrochemical data are shown in Table 2. Selected CV curves are shown in Fig. 5. All redox-active ferrocenyl groups exhibited one-electron transfer processes with formal redox potentials $E_{1/2}$ = 146–148 mV for **Ia-8**, **Ia-12** and $E_{1/2}$ = 79 mV for **Ib-12** *vs.* Fc/Fc^+, which indicates that lengthening of the alkoxy chain has little effect on the formal redox potentials of ferrocene. However, as compared to **Ia-8** and **Ia-12**, the potentials for **Ib-12** cathodically shifted about 70 mV thereby suggesting easy oxidation by loss of an electron for [3] ferrocenophane-containing derivatives. A reasonable explanation is the effect of trimethylene group as an electron donor in [3]ferrocenophane-containing derivative leading to the lower oxidation potential of ferrocene.[36] From Table 2, we found the i_{pc}/i_{pa} ratios approached 1, but the ΔE value was in the range of 143–149 mV indicating a quasi-reversible redox step for studied

Table 2 CV data of 10^{-3} M solutions of selected compounds in CH_2Cl_2 containing 0.1 M $TBAPF_6$ as supporting electrolyte at 100 mV s^{-1} scan rate. Potentials are *vs.* Fc/Fc^+

Compd.	E_{pa}[a]/mV	E_{pc}[b]/mV	ΔE[c]/mV	$E_{1/2}$[d]/mV	i_{pa}[e]/μA	i_{pa}/i_{pc}[f]
Ia-8	223	74	149	148	27.4	0.96
Ia-12	217	74	143	146	25.0	0.89
Ib-12	151	6	145	79	29.4	0.99

[a] Anodic peak potential. [b] Cathodic peak potential. [c] $\Delta E = E_{pa} - E_{pc}$. [d] $E_{1/2} = 1/2(E_{pa} + E_{pc})$. [e] Anodic peak current. [f] i_{pc}, cathodic peak current.

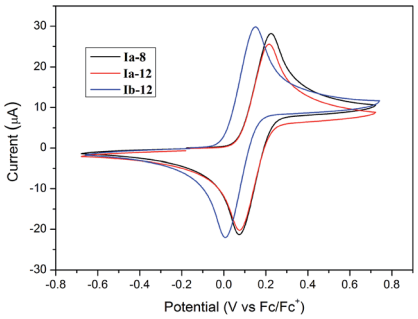

Fig. 5 CV curves of selective compounds **Ia–Ib** in CH_2Cl_2, 0.1 M $TBAPF_6$. Scan rate = 100 mV s^{-1}.

compounds. In addition, as shown in Fig. 6, the redox potentials of **Ib-8** slightly influenced by the scan rate in a range from 10 to 300 mV s^{-1}, and both the anodic and cathodic peak currents are linear to the square root of scan rates, indicating a diffusion-controlled process.[34]

2.3 Thermal behavior

Thermal stability of these compounds was measured by simultaneous thermogravimetric and differential scanning calorimetry (TG-DSC) measurement under N_2. The TG curves of **Ia–Id** are shown in Fig. S1.† From the TG curves, we can see that the decomposition temperatures were somewhat higher for **Ic-8** and **Id-8** (about 300 °C) than for **Ia-8** and **Ib-8** (about 270 °C), which indicated the higher thermal stability of the former.

Mesomorphic properties of these compounds had been investigated. The textural studies of them have been performed using thermal polarizing microscopy (POM) and the thermal analyses have been carried out using DSC. The thermal analyses data of compounds **Ia**, **Ib**, **II** and **III** are presented in Table S2.† As shown in Table S2,† compounds **Ia–Ib** did not display LC behaviors, however, most of them gave rise to crystal to crystal or crystal polymorphic phase transitions upon heating and cooling cycles. For the series of compounds **Ia**, the phase transition temperature of crystal to isotropic liquid lowered gradually with increasing the length of the terminal alkoxy chain from eight to fourteen carbon atoms, but this temperature raised when further lengthening the terminal alkoxy chain to sixteen

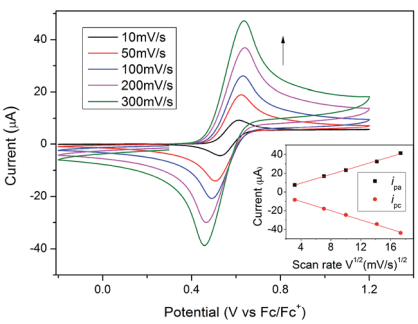

Fig. 6 CV curves and peak currents of **Ib-8** obtained at different scan rates in CH_2Cl_2.

carbon atoms. In addition, this temperature for the series of compounds **Ib** with the same length of terminal alkoxy chain lowered obviously when replacing ferrocene by [3] ferrocenophane.

Compounds **Ia–Ib** were non-mesomorphic. It seems to like that there is unfavourable effect of bulky ferrocene in present system which is disadvantageous to molecule packing, so ferrocene was replaced by a benzene ring or thiophene ring in the following study. Compounds **Ic–Id** with one terminal alkoxy chain on the side of ester group were prepared, and we were pleased to find that they all displayed liquid crystal behaviors and showed similar phase transitions in the heating and cooling cycles. As examples, the DSC curves of **Ic-8** and **Id-8** are shown in Fig. 7. At the beginning of the first heating cycle, crystal to crystal phase transition was observed for **Ic-8**, then an endothermic peak appeared at 167 °C with large enthalpy change of 82.0 kJ mol^{-1} corresponding to the melting point followed by the formation of mesophase with the range of 61 °C. The mesophase exhibited marbled texture as presented in Fig. 8a which was identified by POM.[37] On slow cooling from the isotropic liquid, the enantiotropic mesophase was observed. The droplet texture for **Ic-8**, fourbrush schlieren texture for **Ic-12** and marbled texture for **Ic-14** appeared on cooling as presented in Fig. 8b–d. X-ray diffraction (XRD) experiments were further performed to elucidate the mesomorphic properties. As shown in Fig. 9, the XRD patterns of **Ic-8** presented one diffuse peak in wide-angle region during the heating and cooling cycle after entering into the mesophase, which demonstrated a disordered position of mesogen. Taking into account the DSC, POM and XRD results, this series compounds probably possessed enantiotropic smectic C (SmC) phase.[38] As shown in Table 3, the mesophase ranges (ΔT) in the cooling cycles were 79.1 °C for **Ic-8**, 56.4 °C for **Ic-12** and 51.5 °C for **Ic-14** respectively, which narrowed gradually with increasing the length of the terminal alkoxy chain. The lower homologues **Ic-8** had the widest mesogenic domain and the highest clearing temperature (~229 °C). Similar thermal behaviors were observed in series **Id**. Moreover, for the compound with same length of terminal alkoxy chain, the mesophase range of the series **Id** containing thiophene (91.0 °C for **Id-8**, 66.0 °C for **Id-12** and 58.7 °C for **Id-14**) was wider, and the clearing points of series **Id** were higher

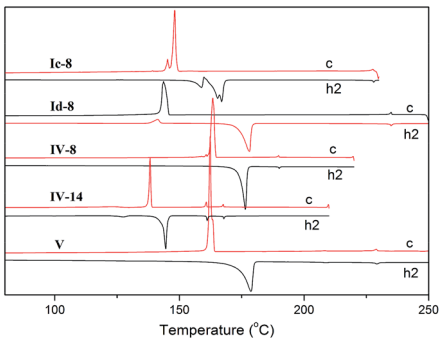

Fig. 7 DSC traces of selected compounds. h2: the second heating, c: the first cooling.

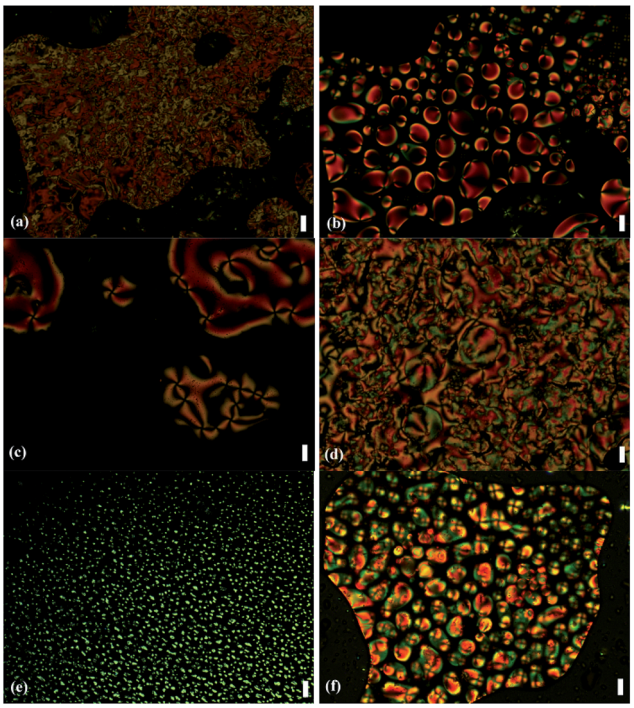

Fig. 8 Polarizing optical microscopy images (20×) (a) **Ic-8** at 195.0 °C on heating, (b) **Ic-8** at 229.8 °C (c) **Ic-12** at 207.4 °C (d) **Ic-14** at 200.4 °C (e) **Id-8** at 232.6 °C (f) **Id-12** at 213.0 °C on cooling. Scale bar, 30 μm.

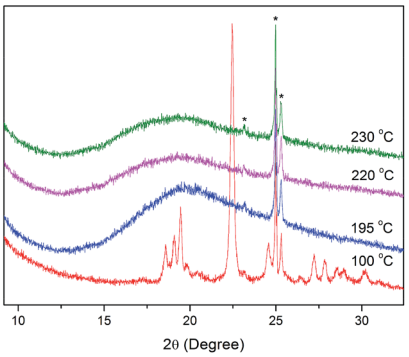

Fig. 9 XRD patterns of compound **Ic-8** on heating 195 °C and cooling 230 °C, 220 °C and 100 °C. Asterisks in the spectrum show the alumina from the sample cell holder.

than those of the series **Ic**. The POM images of **Id-8** at 232.6 °C and **Id-12** at 213.0 °C on cooling were presented in Fig. 8e and f. Therefore, the presence of heteroatom S being more polarizable than carbon resulted in great changes in the corresponding liquid crystalline phases and physical properties of the observed phases.

Compounds **Ic–Id** all exhibited enantiotropic mesomorphic behaviours, but their melting points were high. In order to obtain mesogenic compounds with low melting point, compounds **IIc–IId** with three terminal alkoxy chains were prepared. As shown in Table S2,† the melting points of compounds **IIc-8**, **IIc-14** and **IId-8** are 73.5, 72.7, and 94.1 °C

Table 3 Phase transition temperatures and associated enthalpies of compounds **1–4**

Compd.	Phase transitions[a] °C (ΔH kJ^{-1} mol^{-1}) First heating	Second heating	First cooling	ΔT^b
Ic-8	C_1 71.7 (8.3) C_2 158.2 (6.8) C_3 167.6 (82.0) M 228.7 (0.9) I	C_2 158.8 (16.2) C_3 166.8 (57.5) M 227.9 (1.2) I	I 227.6 (−1.13) M 148.5 (−56.2) C_3 145.3 (−9.5) C_2	79.1
Ic-12	C_1 102.2 (17.6) C_2 128.2 (6.8) C_3 161.1 (78.0) M 207.5 (1.3) I	C 160.7 (72.3) M 205.9 (1.5) I	I 205.2 (−1.31) M 148.8 (−71.2) C	56.4
Ic-14	C_1 113.0 (31.7) C_2 164.4 (86.6) M 201.8 (1.6) I	C_1 61.2 (12.3) C_2 164.2 (82.0) M 201.1 (1.6) I	I 200.3 (−1.3) M 148.8 (−80.1) C_2 66.0 (−11.3) C_1	51.5
Id-8	C 178.8 (97.9) M 236.7 (2.21) I	$C_1$141.4 (−10.4) C_2 177.8 (91.3) M 234.9 (2.04) I	I 234.9 (−1.93) M 143.9 (−71.4) C	91.0
Id-12	C_1 103.6 (32.1) C_2 159.4 (128.9) M 213.8 (2.4) I	C_1 51.4 (5.4) C_2 158.9 (116.5) M 212.9 (2.7) I	I 212.5 (−2.2) M 146.5 (−110.7) C_2 45.4 (−6.3) C_1	66.0
Id-14	C_1 113.8 (31.7) C_2 160.5 (84.5) M 205.3 (1.4) I	C 159.7 (78.0) M 205.3 (1.5) I	I 204.6 (−1.57) M 145.9 (−76.6) C	58.7
IV-8	C_1 123.2 (8.0) C_2 176.0 (54.3) M 190.2 (0.6) I	C_1 176.1 (52.2) M 189.9 (0.6) I	I 189.8 (−0.4) M 163.8 (−49.2) C	26.0
IV-10	C_1 76.5 (15.4) C_2 151.2 (42.5) M 181.1 (0.6) I	C 158.6 (43.9) M 180.8 (0.7) I	I 180.7 (−0.8) M 144.9 (−34.7) C	35.8
IV-12	C_1 82.5 (5.6) C_2 98.8 (8.3) C_3 104.7 (1.8) C_4 146.8 (44.9) M_1 153.0 (0.8) M_2 172.8 (0.9) I	C_1 113.9 (2.8) C_2 147.4 (34.5) M_1 152.84 (0.6) M_2 172.6 (0.8) I	I 172.3 (−0.9) M_2 152.6 (−0.9) M_1 142.6 (−29.9) C	29.7
IV-14	C_1 92.56 (5.5) C_2 109.55 (27.0) C_3 144.1 (43.4) M_1 161.2 (1.9) M_2 167.9 (0.4) I	C_1 127.5 (4.0) C_2 144.3 (37.9) M_1 161.1 (2.0) M_2 167.8 (0.6) I	I 167.6 (−0.8) M_2 160.8 (−1.8) M_1 138.5 (−26.9) C	29.1
V	C 180.4 (40.8) M 235.7 (0.8) I	C 178.4 (38.3) M 229.1 (0.7) I	I 229.1 (−0.5) M 163.3 (−34.8) C	65.8

[a] C: crystal, M: mesophase, I: isotropic liquid. [b] Mesophase range.

respectively, lowering 85–94 °C compared with compounds **Ic-8**, **Ic-14** and **Id-8**. However, compounds **IIc–IId** with three terminal alkoxy chains were non-mesomorphic, but showed either simple melting and freezing process or crystal polymorphic phase transitions in the heating and cooling cycles. From above observations, it seemed likely that increasing the number of long chain was unfavourable for inducing mesomorphism due to increasing the disorder of molecular.

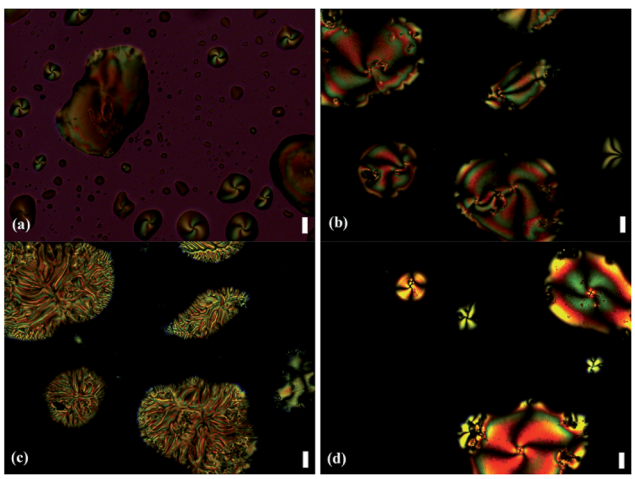

Fig. 10 Polarizing optical microscopy images (20×) (a) **IV-8** at 192.4 °C on heating, (b) **IV-14** at 169.6 °C (c) **IV-14** at 162.7 °C (d) **V** at 239.6 °C on cooling. Scale bar, 30 μm.

To better understand the effect of the position of long chain on the formation of mesophases, compounds **III-8** and **III-14** with terminal alkoxy chain on the side of chalcone were prepared. We were surprised to find that compounds **III-8** and **III-14** showed no liquid crystal behaviours. As shown in Table S2,† compounds **III-8** and **III-14** also displayed crystal polymorphic phase transitions in the heating and cooling cycles, and their melting points (**III-8**, 184.8 °C; **III-14**, 173.6 °C) were slight higher than those of compounds **Ic-8** (167.6 °C) and **Ic-14** (164.4 °C).

Next, we studied the thermal behaviours of compounds **IV–V** with a terminal alkoxy chain at both ends of the molecular. From Table 3, we can see that the melting point of compound **IV-8** (176.0 °C) increased by about 10 °C compared with **1c-8** (167.6 °C), whereas the increase of the length of the flexible chain (**IV-12**, 146.8 °C; **IV-14**, 144.1 °C) resulted in a decrease of the melting point by 15–20 °C compared with **Ic-12** (161.1 °C) and **Ic-14** (164.4 °C). According DSC and POM observation, the series **IV** all showed enantiotropic mesophases but with the narrow mesogenic domains (26–36 °C) and low clearing temperature compared with the series of **Ic**. Upon heating, compounds **IV-8** and **IV-10** having shorter chains exhibited schlieren texture after entering into the mesophase, and showed fourfold brush near the melting point (Fig. 10a). The inversing process was also observed on cooling. However, as shown in Table 3, **IV-12** and **IV-14** having longer chains displayed two mesogenic domains. As an example, on cooling from isotropic of **IV-14**, fourbrush schlieren texture was observed at

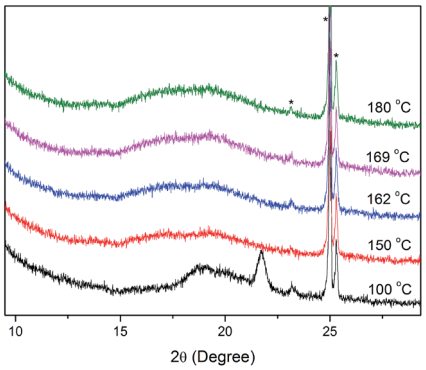

Fig. 11 XRD patterns of compound **IV-14** on cooling. Asterisks in the spectrum show the alumina from the sample cell holder.

169.6 °C as displayed in Fig. 10b and further cooling, dendritic texture were exhibited at 162.7 °C as displayed in Fig. 10c.[39] The XRD patterns of **IV-14** (Fig. 11) presented one diffuse peak during the cooling cycle after entering into the mesophase indicating the possibility of SmC phase.

The increase of the length of the mesogenic unit by replacement benzene ring with naphthalene ring (compound **V**) resulted in both an increase of the clearing point by about 46 °C compared with its analogue, compound **IV-8**, and in an increase of the SmC mesophase domain (by about 40 °C), but the melting point changed slightly. Fig. 10d showed the POM image of **V** at 239.6 °C on cooling. Thus, the lengthening the rigid core may favour a better packing of the molecules which was beneficial to exhibiting liquid crystal properties.

3 Conclusion

In summary, we have synthesized 23 azobenzene compounds involving chalcone and ester linkages. The compounds containing ferrocene exhibit good electrochemical properties. Investigations of liquid crystal properties indicated that the compounds containing ferrocene (**Ia–Ib** series) and the compounds with three (**IIc–IId** series) or no (**III** series) terminal alkoxy chains on the side of ester group all showed no liquid crystal behaviours. However, the compounds with a terminal alkoxy chain on the side of ester group (**Ic–Id** series) or a terminal alkoxy chain at both ends of the molecular (**IV–V** series) exhibited enantiotropic SmC phases. The replacement benzene ring with naphthalene ring results in both an increase of the clearing point and in an increase of the mesophase domain. Some of these azo molecules underwent photoisomerization under UV light. Very long thermal back relaxation has potential advantage in the creation of optical storage devices.

4 Experimental

4.1 Materials and measurements

Detailed procedures of synthesis and characterization of compounds **VIa–VIe** were described in ESI.† Acyl chloride **VII** was prepared according to reported procedures.[25] IR spectra were recorded as KBr pellets on a Bruker-ALPHA spectrometer. NMR spectra were recorded on an Avance 500 Bruker (500 MHz) spectrometer using tetramethylsilane as internal standard. HRMS spectra were recorded on a Bruker ultrafleXtreme MALDI-TOF/TOF mass spectrometer. Elemental analysis was performed on a Perkins-Elmer 2400 elemental analyser. Electronic absorption spectra were recorded on Shimadzu UV2600 spectrophotometer. Thermal stability was measured by EXSTAR TG/DTA7300 simultaneous TG-DSC measurement under N_2. DSC thermographs were obtained on a METTLER TOLEDO DSC3 at a heating rate of 10 °C min^{-1} under nitrogen flow. Powder XRD experiments were conducted using a D8 ADVANCE equipped with a LynxEye detector, CuKα radiation source, and graphite monochromator, $\lambda = 1.54$ Å. CV experiments were recorded on AUTOLAB PGSTAT302 voltammetric analyzer and performed at room temperature in dry CH_2Cl_2 solutions with the concentration of 10^{-3} M containing 0.1 M $TBAPF_6$ as a supporting electrolyte. A three-electrode configuration consisting of a glassy carbon working electrode, a Pt wire counter electrode, and an Ag/AgCl (with a saturated KCl solution) couple reference electrode was used. The Fc/Fc^+ couple was used as internal reference and showed a peak at +0.484 V *vs.* Ag/AgCl. Prior to experiments, the system was purged with purified nitrogen gas to exclude dissolved oxygen from the solution.

4.2 General procedure for the synthesis of compounds I–V

Compound **VI** (0.45 mmol) was redissolved in dry pyridine (2 mL), to which acyl chloride **VII** (0.5 mmol) in dry pyridine (2 mL) was added dropwise at −5 °C. The reaction was stirred for 4 h at room temperature. The solvent was removed by distillation at reduced pressure and the residue was separated by silica gel column chromatography using CH_2Cl_2/petroleum ether as eluent. The second fraction was the desired product, which was recrystallized from CH_2Cl_2/methanol to afford the pure compounds **I–V** (Scheme 1).

Ia-8. Yield 67%, mp 172–178 °C, $R_f = 0.117$ (CH_2Cl_2 : petroleum ether = 2 : 1); IR (KBr, ν, cm^{-1}): 3102, 2950, 2919, 2853, 1733, 1654, 1592, 1509, 1315, 1261, 1074, 979; ^{1}H NMR (500 MHz, $CDCl_3$) (δ ppm): 8.17–8.13 (m, 4H, C_6H_4), 8.06–8.00 (m, 4H, C_6H_4), 7.81 (d, J = 15.0 Hz, 1H, CH), 7.41 (d, J = 8.5 Hz, 2H, C_6H_4), 7.17 (d, J = 15.0 Hz, 1H, CH), 7.00 (d, J = 9.0 Hz, 2H, C_6H_4), 4.63 (d, J = 2.0 Hz, 2H, FcH), 4.52 (d, J = 2.0 Hz, 2H, FcH), 4.21 (s, 5H, FcH),

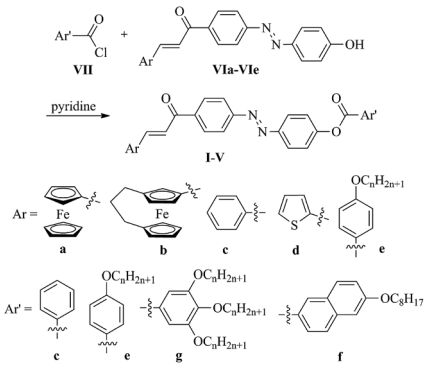

Scheme 1 Synthesis of compounds I–V.

4.06 (t, J = 6.5 Hz, 2H, OCH_2), 1.88–1.78 (m, 2H, CH_2), 1.52–1.44 (m, 2H, CH_2), 1.37–1.45 (m, 8H, CH_2), 0.90 (t, J = 7.0 Hz, 3H, CH_3); ^{13}C NMR (125 MHz, $CDCl_3$) (δ ppm): 188.97, 164.62, 163.82, 154.62, 153.76, 150.23, 147.55, 132.45, 129.49, 124.49, 122.98, 122.65, 121.17, 114.46, 72.74, 72.30, 70.58, 69.67, 68.44, 31.86, 29.38, 29.28, 26.04, 22.71, 14.16; HRMS, MALDI$^+$, m/z: calcd for $C_{40}H_{40}FeN_2O_4$: [M^+] 668.2337, found: 668.2333.

Ia-10. Yield 71%, mp 182–184 °C, R_f = 0.263 (CH_2Cl_2 : petroleum ether = 3 : 1); IR (KBr, ν, cm^{-1}): 3051, 2922, 2851, 1731, 1654, 1590, 1512, 1316, 1267, 1104, 978; ^{1}H NMR (500 MHz, $CDCl_3$) (δ ppm): 8.16 (d, J = 8.5 Hz, 2H, C_6H_4), 8.12 (d, J = 7.0 Hz, 2H, C_6H_4), 8.05 (d, J = 8.5 Hz, 2H, C_6H_4), 8.01 (d, J = 8.0 Hz, 2H, C_6H_4), 7.75 (d, J = 14.0 Hz, 1H, CH), 7.40 (d, J = 9.0 Hz, 2H, C_6H_4), 7.13 (d, J = 14 Hz, 1H, CH), 6.99 (d, J = 9.0 Hz, 2H, C_6H_4), 4.76 (s, 2H, FcH), 4.64 (s, 2H, FcH), 4.33 (s, 5H, FcH), 4.06 (t, J = 6.5 Hz, 2H, OCH_2), 1.86–1.80 (m, 2H, CH_2), 1.51–1.45 (m, 2H, CH_2), 1.41–1.19 (m, 12H, CH_2), 0.89 (t, J = 7.0 Hz, 3H, CH_3); ^{13}C NMR (125 MHz, $CDCl_3$) (δ ppm): 189.09, 164.59, 163.78, 154.58, 153.72, 150.19, 147.54, 132.41, 129.39, 124.45, 122.93, 122.61, 121.13, 119.02, 114.42, 71.61, 69.90, 69.16, 68.40, 31.91, 29.57, 29.36, 29.11, 26.00, 22.70, 14.14; HRMS, MALDI$^+$, m/z: calcd for $C_{42}H_{44}FeN_2O_4$: [M^+] 696.2651, found: 696.2648.

Ia-12. Yield 66.5%, mp 164–168 °C, R_f = 0.27 (CH_2Cl_2 : petroleum ether = 3 : 1); IR (KBr, ν, cm^{-1}): 3088, 2920, 2850, 1728, 1653, 1602, 1510, 1314, 1256, 1070, 979; ^{1}H NMR (500 MHz, $CDCl_3$) (δ ppm): 8.16 (d, J = 8.5 Hz, 2H, C_6H_4), 8.12 (d, J = 8.0 Hz, 2H, C_6H_4), 8.05 (d, J = 8.5 Hz, 2H, C_6H_4), 8.01 (s, 2H, C_6H_4), 7.73 (b, 1H, CH), 7.40 (d, J = 8.5 Hz, 2H, C_6H_4), 7.14 (b, 1H, CH), 6.99 (d, J = 8.5 Hz, 2H, C_6H_4), 4.83 (s, 2H, FcH), 4.69 (s, 2H, FcH), 4.37 (s, 5H, FcH), 4.06 (t, J = 6.5 Hz, 2H, OCH_2), 1.84–1.80 (m, 2H, CH_2), 1.49–1.46 (m, 2H, CH_2), 1.37–1.20 (m, 16H, CH_2), 0.88 (t, J = 6.5 Hz, 3H, CH_3); ^{13}C NMR (125 MHz, $CDCl_3$) (δ ppm): 188.98, 164.59, 163.78, 154.57, 153.72, 150.19, 146.41, 132.41, 129.55, 124.45, 122.99, 122.61, 121.13, 114.41, 71.17, 69.97, 69.63, 68.40, 31.94, 29.63, 29.37, 22.71, 14.14; HRMS, MALDI$^+$, m/z: calcd for $C_{44}H_{48}FeN_2O_4$: [M^+] 724.2964, found: 724.2966.

Ia-14. Yield 72.3%, mp 172–176 °C, R_f = 0.27 (CH_2Cl_2 : petroleum ether = 3 : 1); IR (KBr, ν, cm^{-1}): 3094, 2921, 2849, 1732, 1654, 1590, 1512, 1316, 1269, 1077, 977; ^{1}H NMR (500 MHz, $CDCl_3$) (δ ppm): 8.16 (d, J = 8.5 Hz, 2H, C_6H_4), 8.13 (d, J = 8.0 Hz, 2H, C_6H_4), 8.05 (d, J = 8.5 Hz, 2H, C_6H_4), 8.01 (d, J = 8.0 Hz, 2H, C_6H_4), 7.79 (d, J = 15.0 Hz, 1H, CH), 7.40 (d, J = 8.5 Hz, 2H, C_6H_4), 7.17 (d, J = 15.0 Hz, 1H, CH), 6.98 (d, J = 8.5 Hz, 2H, C_6H_4), 4.66 (s, 2H, FcH), 4.55 (s, 2H, FcH), 4.23 (s, 5H, FcH), 4.06 (t, J = 6.5 Hz, 2H, OCH_2), 1.86–1.80 (m, 2H, CH_2), 1.49–1.45 (m, 2H, CH_2), 1.37–1.26 (m, 20H, CH_2), 0.88 (t, J = 6.5 Hz, 3H, CH_3); ^{13}C NMR (125 MHz, $CDCl_3$) (δ ppm): 189.00, 164.59, 163.78, 154.58, 153.71, 150.18, 147.55, 132.41, 129.45, 124.45, 122.93, 122.61, 119.12, 114.41, 70.51, 69.63, 69.34, 68.40, 31.94, 29.64, 29.38, 29.11, 26.00, 22.71, 14.15; HRMS, MALDI$^+$, m/z: calcd for $C_{46}H_{52}FeN_2O_4$: [M^+] 752.3277, found: 752.3278.

Ia-16. Yield 73%, mp 168–170 °C, R_f = 0.275 (CH_2Cl_2 : petroleum ether = 3 : 1); IR (KBr, ν, cm^{-1}): 3094, 2950, 2920, 2854, 1732, 1653, 1592, 1509, 1316, 1260, 1074, 979; ^{1}H NMR (500 MHz, $CDCl_3$) (δ ppm): 8.16 (d, J = 8.5 Hz, 2H, C_6H_4), 8.11 (b, 2H, C_6H_4), 7.05 (d, J = 8.5 Hz, 2H, C_6H_4), 8.01 (b, 2H, C_6H_4), 7.71 (b, 1H, CH), 7.40 (d, J = 8.5 Hz, 2H, C_6H_4), 7.14 (s, 1H, CH), 6.98 (d, J = 8.5 Hz, 2H, C_6H_4), 4.84 (s, 2H, FcH), 4.71 (s, 2H, FcH), 4.39 (s, 5H, FcH), 4.05 (t, J = 6.5 Hz, 2H, OCH_2), 1.85–1.80 (m, 2H, CH_2), 1.49–1.46 (m, 2H, CH_2), 1.37–1.20 (m, 24H, CH_2), 0.88 (t, J = 6.7 Hz, 3H, CH_3); ^{13}C NMR (125 MHz, $CDCl_3$) (δ ppm): 188.94, 164.58, 163.78, 154.57, 153.72, 151.74–151.56, 150.18–149.98, 132.41, 124.45, 122.98, 122.61, 121.13, 114.41, 68.41, 31.95, 29.71, 29.64, 29.38, 26.00, 22.71, 14.15; HRMS, MALDI$^+$, m/z: calcd for $C_{48}H_{56}FeN_2O_4$: [M^+] 780.3590, found: 780.3585.

Ib-8. Yield 77.2%, mp 142–145 °C, R_f = 0.23 (CH_2Cl_2 : petroleum ether = 3 : 1); IR (KBr, ν, cm^{-1}): 3078.37, 2926.80, 2852.78, 1731.00, 1650.52, 1603.11, 1509.38, 1260.60, 1070.15, 976.68; ^{1}H NMR (500 MHz, $CDCl_3$) (δ ppm): 8.17 (d, J = 8.5 Hz, 2H, C_6H_4), 8.11 (d, J = 8.5 Hz, 2H, C_6H_4), 8.05 (d, J = 8.5 Hz, 2H, C_6H_4), 8.00 (s, 2H, C_6H_4), 7.82 (b, 1H, CH), 7.40 (d, J = 8.5 Hz, 2H, C_6H_4), 7.05 (b, 1H, CH), 6.99 (d, J = 8.5 Hz, 2H, C_6H_4), 4.65 (b, 2H, FcH), 4.51–4.29 (m, 3H, FcH), 4.17–4.04 (m, 3H, FcH, OCH_2), 3.93 (s, 1H, FcH), 2.02–1.62 (m, 8H, CH_2), 1.52–1.45 (m, 2H, CH_2), 1.42–1.24 (m, 8H, CH_2), 0.90 (t, J = 6.5 Hz, 3H, CH_3); ^{13}C NMR (125 MHz, $CDCl_3$) (δ ppm): 188.66, 164.58, 163.77, 162.62, 154.38, 153.66, 150.20, 149.61, 147.76, 147.73, 147.70, 132.41, 132.41, 131.16, 129.31, 125.80, 124.48, 124.41, 123.11, 123.03, 122.60, 121.13, 114.41, 89.67, 86.60, 73.49, 73.47, 70.78, 69.99, 68.40, 34.85, 31.82, 29.71, 29.34, 29.24, 29.01, 26.00, 24.54, 24.09, 22.67, 14.13; HRMS, ESI m/z: calcd for $C_{43}H_{44}FeN_2O_4$: $[M]^+$ 708.2646, found: 708.2631.

Ib-12. Yield 78.5%, mp 140–144 °C, R_f = 0.215 (CH_2Cl_2 : petroleum ether = 3 : 1); IR (KBr, ν, cm^{-1}): 3124.18, 2923.63, 2853.37, 1727.16, 1648.34, 1602.12, 1510.01, 1258.84, 1075.98, 975.69. ^{1}H NMR (500 MHz, $CDCl_3$) (δ ppm): 8.16 (d, J = 8.5 Hz, 2H, C_6H_4), 8.11 (d, J = 6.5 Hz, 2H, C_6H_4), 8.06 (d, J = 8.5 Hz, 2H, C_6H_4), 8.00 (d, J = 7.0 Hz, 2H, C_6H_4), 7.76 (d, J = 14.0 Hz, 1H, CH), 7.41 (d, J = 8.5 Hz, 2H, C_6H_4), 7.05 (d, J = 14.0 Hz, 1H, CH), 7.00 (d, J = 9.0 Hz, 2H, C_6H_4), 4.54 (s, 2H, FcH), 4.36 (s, 1H, FcH), 4.33 (s, 1H, FcH), 4.28 (s, 1H, FcH), 4.07 (t, J = 6.5 Hz, 3H, OCH_2), 3.90 (s, 1H, FcH), 2.06–1.89 (m, 6H, CH_2), 1.86–1.80 (m, 2H, CH_2), 1.51–1.45 (m, 2H, CH_2), 1.37–1.25 (m, 16H, CH_2), 0.89 (t, J = 6.5 Hz, 3H, CH_3); ^{13}C NMR (125 MHz, $CDCl_3$) (δ ppm): 189.04, 164.53, 163.79, 154.46, 153.70, 150.24, 147.64, 147.64, 140.56, 132.39, 129.30, 124.39, 122.89, 122.55, 114.43, 89.63, 86.58, 73.44, 73.43, 70.80, 70.24, 70.22, 70.20, 70.06, 68.41, 34.83, 31.91, 29.61, 29.35, 29.10, 25.99, 24.55, 24.11, 22.67, 14.08; HRMS, ESI m/z: calcd for $C_{47}H_{52}FeN_2O_4$: $[M]^+$ 764.3272, found: 764.3263.

Ic-8. Yield 72.5%, mp 158–165 °C, R_f = 0.25 (CH_2Cl_2 : petroleum ether = 2 : 1); IR (KBr, ν, cm^{-1}): 3052, 2953, 2922, 2853, 1729, 1656, 1605, 1573, 1466, 1306, 1259, 1066, 842; ^{1}H NMR (500 MHz, $CDCl_3$) (δ ppm): 8.19 (d, J = 8.5 Hz, 2H, C_6H_4), 8.17 (d, J = 9.0 Hz, 2H, C_6H_4), 8.07 (d, J = 8.5 Hz, 2H, C_6H_4), 8.03 (d, J = 8.5 Hz, 2H, C_6H_4), 7.86 (d, J = 15.5 Hz, 1H, CH), 7.69–7.68 (m, 2H, C_6H_5), 7.58 (d, J = 15.5 Hz, 1H, CH), 7.45–7.44 (m, 3H, C_6H_5), 7.42 (d, J = 9.0 Hz, 2H, C_6H_4), 6.99 (d, J = 8.5 Hz, 2H, C_6H_4), 4.06 (t, J = 6.5 Hz, 2H, OCH_2), 1.86–1.81 (m, 2H, CH_2), 1.51–1.47 (m, 2H, CH_2), 1.42–1.23 (m, 8H, CH_2), 0.90 (t, J = 7.0 Hz, 3H, CH_3); ^{13}C NMR (125 MHz, $CDCl_3$) (δ ppm): 189.85, 164.58, 163.79, 154.83, 153.79, 150.17, 145.34, 139.69, 134.81, 132.41, 130.75, 129.59, 129.04, 128.57, 124.49, 123.01, 122.62, 121.99, 121.12, 114.42, 68.40, 31.82, 29.34, 29.23, 29.11, 26.00,

22.67, 14.12; HRMS, MALDI$^+$ *m*/*z*: calcd for $C_{36}H_{37}N_2NaO_4$: $[M + Na]^+$ 583.2567, found: 583.2560.

Ic-12. Yield 75.3%, mp 150–156 °C, $R_f = 0.277$ (CH_2Cl_2 : petroleum ether = 2 : 1); IR (KBr, ν, cm^{-1}): 3052, 2953, 2821, 2853, 1729, 1656, 1605, 1578, 1495, 1306, 1259, 1066, 842; ^{1}H NMR (500 MHz, $CDCl_3$) (δ ppm): 8.18 (d, $J = 8.5$ Hz, 2H, C_6H_4), 8.16 (d, $J = 9.0$ Hz, 2H, C_6H_4), 8.05 (d, $J = 9.0$ Hz, 2H, C_6H_4), 8.02 (d, $J = 8.5$ Hz, 2H, C_6H_4), 7.85 (d, $J = 15.5$ Hz, 1H, CH), 7.69–7.68 (m, 2H, C_6H_5), 7.58 (d, $J = 15.5$ Hz, 1H, CH), 7.45–7.44 (m, 3H, C_6H_5), 7.42 (d, $J = 9.0$ Hz, 2H, C_6H_4), 7.00 (d, $J = 9.0$ Hz, 2H, C_6H_4), 4.06 (t, $J = 6.5$ Hz, 2H, OCH_2), 1.86–1.80 (m, 2H, CH_2), 1.48–1.45 (m, 2H, CH_2), 1.37–1.26 (m, 16H, CH_2), 0.89 (t, $J = 7.0$ Hz, 3H, CH_3); ^{13}C NMR (125 MHz, $CDCl_3$) (δ ppm): 189.84, 164.57, 163.79, 154.82, 153.79, 150.16, 145.34, 139.68, 134.81, 132.41, 130.75, 129.59, 129.04, 128.58, 124.49, 123.01, 122.62, 121.98, 121.12, 114.42, 68.40, 31.94, 29.67, 29.65, 29.60, 29.57, 29.37, 29.11, 26.00, 22.71, 14.15; HRMS, MALDI$^+$ *m*/*z*: calcd for $C_{40}H_{45}N_2O_4$: $[M + H]^+$ 617.3379, found: 617.3350. Elemental analysis: calcd for $C_{40}H_{44}N_2O_4$: C 77.89, H 7.19, N 4.54%; found: C 77.73, H 7.55, N 4.33%.

Ic-14. Yield 76.9%, mp 162–164 °C, $R_f = 0.28$ (ethyl acetate : petroleum ether = 1 : 20); IR (KBr, ν, cm^{-1}): 3125.77, 2954.43, 2849.44, 1736.54, 1657.86, 1608.91, 1575.47, 1497.17, 1307.46, 1259.58, 1082.75, 842.04; ^{1}H NMR (500 MHz, $CDCl_3$) (δ ppm): 8.18 (d, $J = 9.0$ Hz, 2H, C_6H_4), 8.16 (d, $J = 9.0$ Hz, 2H, C_6H_4), 8.06 (t, $J = 9.0$ Hz, 2H, C_6H_4), 8.04 (t, $J = 8.5$ Hz, 2H, C_6H_4), 7.88 (d, $J = 15.5$ Hz, 1H, CH), 7.69–7.68 (m, 2H, C_6H_5), 7.60 (d, $J = 15.5$ Hz, 1H, ArH), 7.42–7.44 (m, 3H, C_6H_5), 7.40 (d, $J = 9.0$ Hz, C_6H_4), 7.00 (d, $J = 9.0$ Hz, 2H, C_6H_4), 4.06 (t, $J = 6.5$ Hz, 2H, OCH_2), 1.86–1.80 (m, 2H, CH_2), 1.51–1.45 (m, 2H, CH_2), 1.37–1.26 (m, 20H, CH_2), 0.88 (t, $J = 7.0$ Hz, 3H, CH_3); ^{13}C NMR (125 MHz, $CDCl_3$) (δ ppm): 189.86, 164.58, 163.79, 153.79, 145.35, 139.69, 134.80, 132.42, 130.75, 129.59, 129.04, 128.58, 124.49, 123.01, 122.63, 121.98, 114.42, 68.40, 31.94, 29.71, 29.69, 29.61, 29.38, 29.11, 26.00, 22.71, 14.15; HRMS, MALDI$^+$ *m*/*z*: calcd for $C_{42}H_{49}N_2O_4$: $[M + H]^+$ 645.3692, found: 645.3668.

Id-8. Yield 75.7%, mp 176–179 °C, $R_f = 0.27$ (CH_2Cl_2 : petroleum ether = 2 : 1); IR (KBr, ν, cm^{-1}): 3105, 2925, 2853, 1731, 1647, 1602, 1567, 1494, 1315, 1257, 1074, 844; ^{1}H NMR (500 MHz, $CDCl_3$) (δ ppm): 8.17 (d, $J = 8.5$ Hz, 4H, C_6H_4), 8.05 (d, $J = 8.5$ Hz, 2H, C_6H_4), 8.01 (d, $J = 8.5$ Hz, 2H, C_6H_4), 7.98 (d, $J = 15.5$ Hz, 1H, CH), 7.46 (d, $J = 5.0$ Hz, 1H, TpH), 7.41–7.37 (m, 4H, C_6H_4), 7.12 (m, 1H, TpH), 6.99 (d, $J = 8.5$ Hz, 2H, C_6H_4), 4.06 (t, $J = 6.5$ Hz, 2H, CH_2), 1.87–1.80 (m, 2H, CH_2), 1.50–1.46 (m, 2H, CH_2), 1.41–1.24 (m, 8H, CH_2), 0.90 (t, $J = 7.0$ Hz, 3H, CH_3); ^{13}C NMR (125 MHz, $CDCl_3$) (δ ppm): 189.17, 164.56, 163.79, 154.81, 153.78, 152.56, 140.34, 137.68, 132.41, 129.48, 129.12, 128.45, 124.49, 123.01, 122.62, 114.42, 68.40, 31.82, 29.34, 29.24, 29.11, 26.00, 22.67, 14.12; HRMS, MALDI$^+$ *m*/*z*: calcd for $C_{34}H_{35}N_2O_4S$: $[M + H]^+$ 567.2318, found: 567.2299.

Id-12. Yield 76%, mp 149–158 °C, $R_f = 0.29$ (CH_2Cl_2 : petroleum ether = 2 : 1); IR (KBr, ν, cm^{-1}): 3128, 2954, 2919, 2849, 1736, 1652, 1596, 1510, 1469, 1289, 1260, 1081, 844; ^{1}H NMR (500 MHz, $CDCl_3$) (δ ppm): 8.17 (d, $J = 8.5$ Hz, 4H, C_6H_4), 8.05 (d, $J = 8.5$ Hz, 2H, C_6H_4), 8.02 (d, $J = 8.5$ Hz, 2H, C_6H_4), 7.98 (d, $J = 15.5$ Hz, 1H, CH), 7.45 (d, $J = 5$ Hz, 1H, TpH), 7.41–7.37 (m, 4H, CH, TpH, C_6H_4), 7.12 (t, $J = 4.5$ Hz, 1H, TpH), 7.00 (d, $J = 9.0$ Hz, 2H, C_6H_4), 4.05 (t, $J = 6.5$ Hz, 2H, OCH_2), 1.85–1.80 (m, 2H, CH_2), 1.51–1.45 (m, 2H, CH_2), 1.37–1.27 (m, 16H, CH_2), 0.89 (t, $J = 7.0$ Hz, 3H, CH_3); ^{13}C NMR (125 MHz, $CDCl_3$) (δ ppm): 189.15, 164.57, 163.79, 154.81, 153.78, 150.16, 140.34, 139.61, 137.66, 132.41, 129.48, 129.12, 128.46, 124.48, 123.01, 122.61, 121.12, 120.65, 114.41, 68.40, 31.94, 29.67, 29.61, 29.58, 29.37, 29.11, 26.00, 22.71, 14.14; HRMS, MALDI$^+$ *m*/*z*: calcd for $C_{38}H_{43}N_2O_4S$: $[M + H]^+$ 623.2944, found 623.2926; elemental analysis: calcd for $C_{38}H_{42}N_2O_4S$: C 73.28, H 6.80, N 4.50%; found: C 72.89, H 6.76, N 4.43%.

Id-14. Yield 73%, mp 158–160 °C, $R_f = 0.305$ (CH_2Cl_2 : petroleum ether = 2 : 1); IR (KBr, ν, cm^{-1}): 3078, 2954, 2918, 2849, 1735, 1652, 1596, 1510, 1469, 1290, 1259, 1081, 852; ^{1}H NMR (500 MHz, $CDCl_3$) (δ ppm): 8.17 (d, $J = 8.5$ Hz, 4H, C_6H_4), 8.05 (d, $J = 8.5$ Hz, 2H, C_6H_4), 8.02 (d, $J = 8.5$ Hz, 2H, C_6H_4), 7.98 (d, $J = 15.5$ Hz, 1H, CH), 7.45 (d, $J = 5$ Hz, 1H, TpH), 7.41–7.37 (m, 4H, CH, TpH, C_6H_4), 7.12 (t, $J = 4.5$ Hz, 1H, TpH), 7.00 (d, $J = 9.0$ Hz, 2H, C_6H_4), 4.06 (t, $J = 6.5$ Hz, 2H, ArH), 1.86–1.80 (m, 2H, CH_2), 1.49–1.47 (m, 2H, CH_2), 1.37–1.27 (m, 20H, CH_2), 0.88 (t, $J = 7.0$ Hz, 3H, CH_3); ^{13}C NMR (125 MHz, $CDCl_3$) (δ ppm): 189.16, 164.58, 163.78, 154.80, 153.78, 150.16, 140.34, 137.68, 132.41, 129.49, 129.13, 128.46, 124.49, 123.01, 122.62, 120.64, 114.41, 68.40, 31.95, 29.69, 29.67, 29.61, 29.57, 29.38, 29.11, 26.00, 22.72, 14.15; HRMS, MALDI$^+$ *m*/*z*: calcd for $C_{40}H_{47}N_2O_4S$: $[M + H]^+$ 651.3257, found: 651.3243; elemental analysis: calcd for $C_{40}H_{46}N_2O_4S$: C 73.81%, H 7.12, N 4.30%; found: C 73.65, H 7.11, N 4.24%.

IIc-8. Yield 53.1%, mp 71–73 °C, $R_f = 0.2$ (CH_2Cl_2 : petroleum ether : ethyl acetate = 2 mL : 1 mL : 20 μL); IR (KBr, ν, cm^{-1}): 3066, 2923, 2853, 2360, 1729, 1656, 1595, 1569, 1496, 1193, 1033, 983; ^{1}H NMR (500 MHz, $CDCl_3$) (δ ppm): 8.19 (d, $J = 8.5$ Hz, 2H), 8.06 (d, $J = 8.5$ Hz, 2H), 8.04 (d, $J = 8.5$ Hz, 2H), 7.87 (d, $J = 15.5$ Hz, 1H), 7.70–7.67 (m, 2H), 7.59 (d, $J = 15.5$ Hz, 1H), 7.47–7.38 (m, 7H), 4.11–4.03 (m, 6H), 1.87–1.76 (m, 6H), 1.53–1.47 (m, 6H), 1.38–1.26 (m, 24H), 0.91–0.87 (m, 9H); ^{13}C NMR (125 MHz, $CDCl_3$) (δ ppm): 189.82, 164.71, 163.66, 154.76, 153.70, 153.34, 153.04, 151.57, 150.58, 150.34, 150.24, 147.02, 145.37, 143.27, 139.75, 134.79, 130.76, 129.59, 129.03, 128.57, 124.52, 123.42, 123.04, 122.54, 122.19, 121.95, 111.07, 108.64, 74.17, 73.63, 69.31, 31.92, 31.68, 31.88, 31.87, 31.84, 31.82, 30.31, 30.20, 29.52, 29.47, 29.43, 29.36, 29.34, 29.31, 29.30, 29.27, 26.09, 26.02, 26.01, 22.69, 14.12. HRMS, MALDI$^+$ *m*/*z*: calcd for $C_{52}H_{68}N_2NaO_6$: $[M + Na]^+$ 839.4975, found: 839.4939.

IIc-14. Yield 53.6%, mp 87–90 °C, $R_f = 0.29$ (CH_2Cl_2 : petroleum ether : ethyl acetate = 3 mL : 1 mL : 20 μL); IR (KBr, ν, cm^{-1}): 3063, 2920, 2850, 1744, 1658, 1576, 1495, 1261, 1011, 879.80; ^{1}H NMR (500 MHz, $CDCl_3$) (δ ppm): 8.19 (d, $J = 8.5$ Hz, 2H), 8.06 (d, $J = 8.5$ Hz, 2H), 8.03 (d, $J = 8.5$ Hz, 2H), 7.87 (d, $J = 15.5$ Hz, 1H), 7.70–7.68 (m, 2H), 7.59 (d, $J = 15.5$ Hz, 1H), 7.46–7.43 (m, 5H), 7.38 (s, 1H), 4.12–4.02 (m, 6H), 1.87–1.75 (m, 6H), 1.53–1.45 (m, 6H), 1.40–1.26 (m, 60H), 0.91–0.86 (m, 9H); ^{13}C NMR (125 MHz, $CDCl_3$) (δ ppm): 189.83, 163.67, 154.77, 153.35, 153.04, 151.58, 150.59, 150.35, 147.03, 145.38, 139.76, 134.80, 130.76, 129.59, 129.04, 128.58, 124.52, 123.43, 123.04, 122.60, 122.53, 122.24, 122.02, 111.10, 108.61, 74.31, 74.22, 73.61, 69.32, 69.31, 69.28, 31.96, 31.95, 31.92, 31.84, 31.82, 30.48, 30.35, 30.26, 30.25, 29.58, 29.57, 29.48, 29.46, 29.45, 29.36,

29.35, 29.34, 29.33, 29.26, 26.16, 26.10, 26.08, 26.05, 22.69, 14.12. HRMS, MALDI$^+$ *m*/*z*: calcd for $C_{70}H_{104}N_2NaO_6$: $[M + Na]^+$ 1091.7792, found: 1901.7763.

IId-8. Yield 53.1%, mp 90–91 °C, $R_f = 0.2$ (CH_2Cl_2 : petroleum ether : ethyl acetate = 3 mL : 1 mL : 20 μL); IR (KBr, ν, cm^{-1}): 3072, 2922, 2854, 1727, 1651, 1586, 1498, 1283, 1028, 942; ^{1}H NMR (500 MHz, $CDCl_3$) (δ ppm): 8.17 (d, $J = 8.5$ Hz, 2H), 8.06 (d, $J = 8.5$ Hz, 2H), 8.02 (d, $J = 8.5$ Hz, 2H), 8.00 (d, $J = 15.5$ Hz, 1H), 7.46 (d, $J = 5.0$ Hz, 1H, TpH), 7.44–7.37 (m, 6H), 7.13–7.11 (m, 1H), 4.11–4.04 (m, 6H), 1.87–1.75 (m, 6H), 1.53–1.47 (m, 6H), 1.40–1.26 (m, 24H), 0.91–0.87 (m, 9H); ^{13}C NMR (125 MHz, $CDCl_3$) (δ ppm): 189.11, 164.71, 163.66, 154.77, 153.70, 153.34, 153.04, 151.58, 150.59, 147.02, 143.27, 140.33, 139.65, 137.69, 132.41, 129.49, 129.13, 128.46, 124.52, 123.48, 123.04, 122.64, 122.53, 120.62, 111.08, 108.65, 74.31, 73.63, 69.32, 31.92, 31.83, 30.37, 30.32, 30.21, 29.53, 29.47, 29.44, 29.39, 29.37, 29.35, 29.32, 29.30, 29.27, 26.10, 26.07, 26.03, 26.02, 22.72, 22.69, 14.12. HRMS, MALDI$^+$ *m*/*z*: calcd for $C_{50}H_{66}N_2NaO_6S$: $[M + Na]^+$ 845.4538, found: 845.4539.

III-8. Yield 71%, mp 186–187 °C, $R_f = 0.2$ (CH_2Cl_2 : petroleum ether : ethyl acetate = 3 mL : 1 mL : 20 μL); IR (KBr, ν, cm^{-1}): 3060, 2954, 2922, 2852, 1744, 1658, 1629, 1572, 1511, 1266, 1084, 979; ^{1}H NMR (500 MHz, $CDCl_3$) (δ ppm): 8.24 (d, J = 7.5 Hz, 2H), 8.17 (d, $J = 8.5$ Hz, 2H), 8.07 (d, $J = 8.5$ Hz, 2H), 8.03 (d, $J = 8.5$ Hz, 2H), 7.83 (d, $J = 15.5$ Hz, 1H), 7.68 (t, $J = 7.5$ Hz, 1H), 7.63 (d, $J = 8.5$ Hz, 2H), 7.55 (t, $J = 7.5$ Hz, 2H), 7.45 (d, J = 15.5 Hz, 1H), 7.42 (d, J = 8.5 Hz, 2H), 6.95 (d, $J = 8.5$ Hz, 2H), 4.02 (t, J = 6.5 Hz, 2H), 1.85–1.78 (m, 2H), 1.50–1.44 (m, 2H), 1.38–1.30 (m, 8H), 0.89 (t, $J = 6.8$ Hz, 3H); ^{13}C NMR (125 MHz, $CDCl_3$) (δ ppm): 189.87, 164.83, 161.53, 154.64, 153.52, 150.31, 145.37, 140.15, 133.90, 130.40, 130.29, 129.48, 129.21, 128.70, 127.28, 124.51, 122.97, 122.54, 119.45, 114.99, 68.25, 31.82, 29.35, 29.25, 29.17, 26.03, 22.68, 14.12. HRMS, MALDI$^+$ *m*/*z*: calcd for $C_{36}H_{37}N_2O_4$: $[M + H]^+$ 561.2753, found: 561.2728.

III-14. Yield 70.6%, mp 165–166 °C, R_f = 0.2 (CH_2Cl_2- : petroleum ether : ethyl acetate = 3 mL : 1 mL : 20 μL), IR (KBr, ν, cm^{-1}): 3042, 2954, 2922, 2852, 1744, 1658, 1629, 1572, 1511, 1266, 1084, 979.70; ^{1}H NMR (500 MHz, $CDCl_3$) (δ ppm): 8.24 (d, J = 7.0 Hz, 2H), 8.17 (d, J = 8.5 Hz, 2H), 8.07 (d, J = 8.5 Hz, 2H), 8.03 (d, J = 8.5 Hz, 2H), 7.83 (d, J = 15.5 Hz, 1H), 7.68 (t, J = 7.5 Hz, 1H), 7.62 (d, J = 8.5 Hz, 2H), 7.55 (t, J = 7.5 Hz, 2H), 7.46 (d, J = 15.5 Hz, 1H), 7.42 (d, J = 8.5 Hz, 2H), 6.94 (d, J = 8.5 Hz, 2H), 4.01 (t, J = 6.5 Hz, 2H), 1.84–1.78 (m, 2H), 1.51–1.43 (m, 2H), 1.36–1.26 (m, 20H), 0.88 (t, J = 6.9 Hz, 3H); ^{13}C NMR (125 MHz, $CDCl_3$) (δ ppm): 189.87, 164.83, 161.53, 154.64, 150.31, 145.37, 133.90, 130.35, 129.48, 128.70, 127.28, 124.51, 122.97, 122.54, 119.45, 114.99, 77.28, 77.03, 76.77, 68.25, 31.82, 29.45–29.03, 26.03, 22.68, 14.12. HRMS, MALDI$^+$ *m*/*z*: calcd for $C_{42}H_{49}N_2NaO_4$: $[M + Na]^+$ 667.3506, found: 667.3519.

IV-8. Yield 42.5%, mp 172–177 °C, $R_f = 0.17$ (CH_2Cl_2 : petroleum ether : ethyl acetate = 2 mL : 1 mL : 20 μL); IR (KBr, ν, cm^{-1}): 3072, 2955, 2922, 2851, 1729, 1656, 1597, 1511, 1262, 1070, 985; ^{1}H NMR (500 MHz, $CDCl_3$) (δ ppm): 8.17 (d, J = 8.5 Hz, 4H), 8.06 (d, $J = 9.0$ Hz, 2H), 8.02 (d, $J = 8.5$ Hz, 2H), 7.83 (d, $J = 15.5$ Hz, 1H), 7.63 (d, $J = 8.5$ Hz, 2H), 7.46 (d, $J = 15.5$ Hz, 1H), 7.40 (d, $J = 9.0$ Hz, 2H), 6.99 (d, $J = 9.0$ Hz, 2H), 6.95 (d, J = 8.5 Hz, 2H), 4.06 (t, $J = 6.5$ Hz, 2H), 4.02 (t, $J = 6.5$ Hz, 2H), 1.86–1.78 (m, 4H), 1.50–1.44 (m, 4H), 1.39–1.26 (m, 16H), 0.91–0.88 (m, 6H). ^{13}C NMR (125 MHz, $CDCl_3$) (δ ppm): 189.85, 163.78, 161.52, 154.67, 153.74, 150.17, 145.34, 140.09, 132.41, 130.40, 129.47, 127.28, 124.46, 122.95, 122.61, 121.13, 119.45, 114.99, 114.41, 77.29, 77.03, 76.78, 68.32, 31.82, 29.22, 26.02, 22.68, 14.13. HRMS, MALDI$^+$ *m*/*z*: calcd for $C_{44}H_{53}N_2O_5$: $[M + H]^+$ 689.3954, found: 689.3922.

IV-10. Yield 42.7%, mp 149–150 °C, $R_f = 0.18$ (CH_2Cl_2 : petroleum ether : ethyl acetate = 2 mL : 1 mL : 20 μL); IR (KBr, ν, cm^{-1}): 3064, 2955, 2920, 2851, 1737, 1658, 1628, 1573, 1510, 1258, 1080, 989; ^{1}H NMR (500 MHz, $CDCl_3$) (δ ppm): 8.17 (d, J = 8.0 Hz, 4H), 8.06 (d, $J = 9.0$ Hz, 2H), 8.02 (d, $J = 8.5$ Hz, 2H), 7.83 (d, $J = 15.5$ Hz, 1H), 7.63 (d, $J = 8.5$ Hz, 2H), 7.46 (d, $J = 15.5$ Hz, 1H), 7.40 (d, $J = 8.5$ Hz, 2H), 6.99 (d, $J = 9.0$ Hz, 2H), 6.95 (d, J = 8.5 Hz, 2H), 4.06 (t, $J = 6.5$ Hz, 2H), 4.01 (t, $J = 6.5$ Hz, 2H), 1.86–1.78 (m, 4H), 1.51–1.44 (m, 4H), 1.36–1.28 (m, 24H), 0.90–0.87 (m, 6H); ^{13}C NMR (125 MHz, $CDCl_3$) (δ ppm): 189.86, 163.78, 161.52, 154.67, 153.74, 145.34, 132.41, 130.40, 129.47, 127.28, 124.46, 122.95, 122.61, 121.12, 119.46, 114.99, 114.41, 77.28, 77.03, 76.78, 68.32, 31.91, 29.57, 29.36, 29.14, 26.01, 22.70, 14.14. HRMS, MALDI$^+$ *m*/*z*: calcd for $C_{48}H_{61}N_2O_5$: $[M + H]^+$ 745.4580, found: 745.4545.

IV-12. Yield 43%, mp 147–148 °C, $R_f = 0.20$ (CH_2Cl_2 : petroleum ether : ethyl acetate = 2 mL : 1 mL : 20 μL); IR (KBr, ν, cm^{-1}): 3068, 2955, 2919, 2850, 1737, 1659, 1603, 1573, 1510, 1260, 1081, 989. ^{1}H NMR (500 MHz, $CDCl_3$) (δ ppm): 8.17 (d, J = 8.0 Hz, 4H), 8.05 (d, $J = 9.0$ Hz, 2H), 8.02 (d, $J = 8.5$ Hz, 2H), 7.83 (d, $J = 15.5$ Hz, 1H), 7.63 (d, $J = 8.5$ Hz, 2H), 7.46 (d, $J = 15.5$ Hz, 1H), 7.40 (d, $J = 8.5$ Hz, 2H), 6.99 (d, $J = 9.0$ Hz, 2H), 6.94 (d, J = 8.5 Hz, 2H), 4.06 (t, $J = 6.5$ Hz, 2H), 4.01 (t, $J = 6.5$ Hz, 2H), 1.86–1.78 (m, 4H), 1.51–1.43 (m, 4H), 1.37–1.27 (m, 32H), 0.89 (t, J = 6.5 Hz, 6H); ^{13}C NMR (125 MHz, $CDCl_3$) (δ ppm): 189.85, 164.57, 163.78, 161.52, 154.67, 153.74, 150.17, 145.34, 140.09, 132.41, 130.40, 129.47, 127.28, 124.46, 122.95, 122.61, 121.12, 119.45, 114.98, 114.41, 77.29, 77.03, 76.78, 68.32, 31.94, 29.63, 29.37, 29.14, 26.01, 22.71, 14.15. HRMS, MALDI$^+$ *m*/*z*: calcd for $C_{52}H_{69}N_2O_5$: $[M + H]^+$ 801.5206, found: 801.5189.

IV-14. Yield 42.6%, mp 140–144 °C, $R_f = 0.23$ (CH_2Cl_2 : petroleum ether : ethyl acetate = 2 mL : 1 mL : 20 μL); IR (KBr, ν, cm^{-1}): 3062, 2955, 2918, 2849, 1736, 1659, 1603, 1568, 1258, 1082.04, 978. ^{1}H NMR (500 MHz, $CDCl_3$) *trans* isomer >85% (δ ppm): 8.17 (d, $J = 8.0$ Hz, 4H), 8.05 (d, $J = 8.5$ Hz, 2H), 8.01 (d, J = 8.5 Hz, 2H), 7.82 (d, $J = 16.0$ Hz, 1H), 7.63 (d, $J = 8.5$ Hz, 2H), 7.46 (d, J = 15.5 Hz, 1H), 7.40 (d, $J = 9.0$ Hz, 2H), 6.99 (d, J = 9.0 Hz, 2H), 6.94 (d, $J = 8.5$ Hz, 2H), 4.06 (t, $J = 6.5$ Hz, 2H), 4.01 (t, J = 6.5 Hz, 2H), 1.86–1.78 (m, 4H), 1.51–1.44 (m, 4H), 1.37–1.24 (m, 40H), 0.88 (t, J = 6.5 Hz, 6H). ^{13}C NMR (125 MHz, $CDCl_3$) (δ ppm): 189.84, 164.52 (s), 163.79, 161.57, 154.57, 153.74, 150.17, 145.32, 140.08, 132.38, 130.42, 129.48, 127.31, 124.42, 122.93, 122.59, 121.12, 119.44, 114.95, 114.46, 77.30, 77.04, 76.77, 68.31, 31.96, 29.64, 29.36, 29.14, 26.03, 22.71, 14.14. HRMS, MALDI$^+$ *m*/*z*: calcd for $C_{56}H_{77}N_2O_5$: $[M + H]^+$ 857.5832, found: 857.5812.

V. Yield 42.7%, mp 220–224 °C, $R_f = 0.18$ (CH_2Cl_2 : petroleum ether : ethyl acetate = 2 mL : 1 mL : 20 μL); IR (KBr, ν, cm^{-1}): 3070, 2923, 2852, 1731, 1655, 1598, 1570, 1510, 1246, 1064, 979; ^{1}H NMR (500 MHz, $CDCl_3$) *trans* isomer >70% (δ ppm): 8.76

(s, 1H), 8.33 (d, J = 9.0 Hz, 1H), 8.27 (d, J = 9.0 Hz, 1H), 8.18 (d, J = 8.5 Hz, 3H), 8.09 (d, J = 8.5 Hz, 2H), 8.03 (d, J = 8.5 Hz, 2H), 7.94 (d, J = 9.0 Hz, 1H), 7.84 (d, J = 15.5 Hz, 1H), 7.63 (d, J = 8.5 Hz, 2H), 7.49–7.44 (m, 3H), 7.39 (d, J = 9.0 Hz, 1H), 7.26 (s, 1H), 6.95 (d, J = 8.5 Hz, 2H), 4.24 (t, J = 6.5 Hz, 2H), 4.02 (t, J = 6.5 Hz, 2H), 1.95–1.87 (m, 2H), 1.84–1.78 (m, 2H), 1.58–1.53 (m, 2H), 1.49–1.45 (m, 2H), 1.42–1.27 (m, 16H), 0.90 (t, J = 6.5 Hz, 6H); ^{13}C NMR (125 MHz, $CDCl_3$) (δ ppm): 189.84, 164.79, 161.53, 154.60, 145.36, 140.15, 132.32, 130.40, 129.56, 127.28, 126.84, 124.62, 124.21, 122.98, 122.58, 119.43, 115.58, 114.99, 77.29, 77.03, 76.78, 70.03, 68.25, 31.83, 29.28, 25.99, 22.68, 14.13. HRMS, MALDI$^+$ m/z: calcd for $C_{48}H_{55}N_2O_5$: $[M + H]^+$ 739.4111, found: 739.4108.

Conflicts of interest

There are no conflicts to declare.

Acknowledgements

We thank the National Natural Science Foundation of China (NSFC, 21562032), Natural Science Foundation of Inner Mongolia (2017MS0205) and Research Program of Science and Technology at Universities of Inner Mongolia (NJZZ001) for their generous financial support.

References

1 S. Laschat, A. Baro, N. Steinke, F. Giesselmann, C. Hägele, G. Scalia, R. Judele, E. Kapatsina, S. Sauer, A. Schreivogel and M. Tosoni, *Angew. Chem.*, 2007, **119**, 4916.
2 G. Lee, R. J. Carlton, F. Araoka, N. L. Abbott and H. Takezoe, *Adv. Mater.*, 2013, **25**, 245.
3 A. M. Lowe and N. L. Abbott, *Chem. Mater.*, 2012, **24**, 746.
4 A. D. Price and D. K. Schwartz, *J. Am. Chem. Soc.*, 2008, **130**, 8188.
5 S. Dixit and R. A. Vora, *Mol. Cryst. Liq. Cryst.*, 2015, **623**, 56.
6 Z. Jiang, M. Xu, F. Li and Y. Yu, *J. Am. Chem. Soc.*, 2013, **135**, 16446.
7 G. Hegde, G. Shanker, S. M. Gan, A. R. Yuvaraj, S. Mahmood and U. K. Mandal, *Liq. Cryst.*, 2016, **43**, 1578.
8 J. Wang, Y. Shi, K. Yang, J. Wei and J. Guo, *RSC Adv.*, 2015, **5**, 67357.
9 M. L. Rahman, T. K. Biswas, S. M. Sarkar, M. M. Yusoff, M. N. F. A. Malek and C. Tschierske, *J. Mol. Liq.*, 2015, **202**, 125.
10 I. Niezgoda, J. Jaworska and Z. Galewski, *J. Mol. Liq.*, 2016, **222**, 571.
11 N. G. Nagaveni, M. Gupta, A. Royb and V. Prasad, *J. Mater. Chem.*, 2010, **20**, 9089.
12 N. Trišović, J. Antanasijević, T. Tóth-Katona, M. Kohout, M. Salamonczyk, S. Sprunt, A. Jákli and K. Fodor-Csorba, *RSC Adv.*, 2015, **5**, 64886.
13 N. G. Nagaveni, A. Royb and V. Prasad, *J. Mater. Chem.*, 2012, **22**, 8948.
14 S. H. Ryu, M. Gim, W. Lee, S. W. Choi and D. K. Yoon, *ACS Appl. Mater. Interfaces*, 2017, **9**, 3186.
15 D. Y. Kim, S. A. Lee, H. Kim, S. M. Kim, N. Kimc and K. U. Jeong, *Chem. Commun.*, 2015, **51**, 11080.
16 A. Zep, K. Sitkowska, D. Pociecha and E. Gorecka, *J. Mater. Chem. C*, 2014, **2**, 2323.
17 H. Y. Zhong, L. Chen, R. Yang, Z. Y. Meng, X. M. Ding, X. F. Liu and Y. Z. Wang, *J. Mater. Chem. C*, 2017, **5**, 3306.
18 E. Verploegen, J. Soulages, M. Kozberg, T. Zhang, G. McKinley and P. Hammond, *Angew. Chem., Int. Ed.*, 2009, **48**, 3494.
19 J. Wang, C. Lin, J. Zhang, J. Wei, Y. Song and J. Guo, *J. Mater. Chem. C*, 2015, **3**, 4179.
20 R. Prasath, P. Bhavana, S. W. Ng and E. R. T. Tiekink, *J. Organomet. Chem.*, 2013, **726**, 62.
21 S. Attar, Z. O'Brien, H. Alhaddad, M. L. Golden and A. Calderón-Urrea, *Bioorg. Med. Chem.*, 2011, **19**, 2055.
22 C. A. Calliste, J. C. Le Bail, P. Trouilas, C. Poug, A. J. Chulia and L. J. Doroux, *Anticancer Res.*, 2001, **21**, 3949.
23 X. Wu, E. R. T. Tiekink, I. Kostetski, N. Kocherginsky, A. L. C. Tan, S. B. Khoo, P. Wilairat and M. L. Go, *Eur. J. Pharm. Sci.*, 2006, **27**, 175.
24 P. S. Patil, S. M. Dharmaprakash, K. Ramakrishna and H. K. Fun, *J. Cryst. Growth*, 2007, **303**, 520.
25 H. Zhao, X. Zhu, D. Wang, S. Chen and Z. Bian, *Aust. J. Chem.*, 2015, **68**, 1035.
26 R. L. Coelho, E. Westphal, D. Z. Mezalira and H. Gallardo, *Liq. Cryst.*, 2017, **44**, 405.
27 H. T. Srinivasa and S. Kumar, *Liq. Cryst.*, 2017, **44**, 1506.
28 A. Karuppusamy, V. Ramkumar, P. Kannan, S. Balamurugan and S. M. Said, *Soft Mater.*, 2017, **15**, 132.
29 B. B. Jain and R. B. Patel, *Mol. Cryst. Liq. Cryst.*, 2016, **638**, 27.
30 N. R. Muniya and V. R. Patel, *Mol. Cryst. Liq. Cryst.*, 2016, **638**, 95.
31 A. S. Pandey, R. Dhar, A. S. Achalkumar and C. V. Yelamaggad, *Liq. Cryst.*, 2011, **38**, 775.
32 J. Li, W. Zhang, Y. Zhao and J. Pu, *Adv. Mater. Res.*, 2012, **380**, 326.
33 D. Jayalatha, R. Balamurugan and P. Kannan, *High Perform. Polym.*, 2009, **21**, 139.
34 H. Zhao, X. Zhu, Y. Shang, S. Chen, B. Li and Z. Bian, *RSC Adv.*, 2016, **6**, 34476.
35 C. Selvarasu and P. Kannan, *J. Mol. Struct.*, 2016, **1125**, 234.
36 T. Ogata, K. Oikawa, T. Fujisawa, S. Motoyama, T. Izumi, A. Kasahara and N. Tanaka, *Bull. Chem. Soc. Jpn.*, 1981, **54**, 3723.
37 S. Y. Kim, O. N. Kadkin, E. H. Kim and M. G. Choi, *J. Organomet. Chem.*, 2011, **696**, 2429.
38 G. Casella, V. Causin, F. Rastrelli and G. Saielli, *Liq. Cryst.*, 2016, **43**, 1161.
39 I. Cârlescu, A. M. Scutar, D. Apreutesei, V. Alupei and D. Scutaru, *Liq. Cryst.*, 2007, **34**, 775.